Aeroelastic Tailoring of Helicopter Blades

Donatien Cornette, Benjamin Kerdreux, Yves Gourinat, Guilhem Michon

AEROELASTIC TAILORING OF HELICOPTER BLADES

Donatien Cornette*
EUROCOPTER
Dynamics Department
F-13725 Marignane Cedex, France
Université de Toulouse, ISAE
ICA (Institut Clément Ader)
F-31055, Toulouse, France
Email: donatien.cornette@eurocopter.com

Benjamin Kerdreux
Dynamics department
EUROCOPTER
F-13725, Marignane, France

Yves Gourinat
Guilhem Michon
Université de Toulouse, ISAE
ICA(Institut Clément Ader)
F-31055, Toulouse, France

ABSTRACT

The dynamic loads transmitted from the rotor to the airframe are responsible for vibrations, discomfort and alternate stress of components. A new and promising way to minimize vibration is to reduce dynamic loads at their source by performing an aeroelastic optimization of the rotor.
This optimization is done thanks to couplings between the flapwise-bending motion and the torsion motion. The impact of elastic couplings (composite anisotropy) on the blade dynamic behaviour and on dynamic loads are evaluated in this paper.
Firstly, analytical results, based on a purely linear modal approach, are given to understand the influence of those couplings in terms of frequency placement, aerodynamic lift load and vertical shear modification. Then, those elastic couplings are introduced on a simplified but representative blade (homogeneous beam with constant chord) and results are presented.

NOMENCLATURE

$A_k(r)$ Spanwise distribution of aerodynamic load at the k^{th} harmonic
C_β Aerodynamic damping of flap modes
EI Flap bending stiffness
F_c Centrifugal load
F_z Out-of-plane load applied by all blades on the fuselage
F_z^i Out-of-plane load applied by i^{th} blade on the fuselage
GJ Torsional stiffness
I_s Section polar mass moment of inertia
I_G Section inertia matrix
K_{45} Flapwise-Bending Torsion stiffness
M_b Bending moment
M_t Torsion moment
Q_β, Q_θ Flap and torsion generalized forces
S Blade cross section
R Rotor radius
$T_z^{n\Omega}$ Vertical shear load at the harmonic n
U Total speed of the section
U_z Vertical Deflection
V_G Speed of the section center of gravity
b Blade number
c Blade chord
$\frac{dC_z}{di}$ Lift curve slope
$f_{z,n}$ Out-of-plane load applied by blade on the fuselage at n^{th} harmonic
l_G Chordwise center of gravity offset
n Harmonic number
r Spanwise position
Ω Rotor speed
Ω_s Section angular speed

*Address all correspondence to this author.

α_β Flap mode damping
θ Torsion
ρ Air mass density
μ Blade mass per unit length
μ_β, μ_θ Flap and torsion modal masses
$\nu K_{\beta\theta}$ Aerodynamic coupling between flap and torsion mode
ϕ_β, ϕ_θ Flap mode and torsion mode shapes
ω_β, ω_θ Frequencies of uncoupled flap and torsion modes
$\hat{\omega}_\beta$, $\hat{\omega}_\theta$ Frequencies of structurally coupled modes
$\dot{(\,)}$ Time derivative
$(\,)'$ Spatial derivative
$\underline{(\,)}$ Vectors
$\underline{\underline{(\,)}}$ Matrix

INTRODUCTION

Dynamic loads and vibration reduction systems

Because of the cyclic variation of the blade angle of attack, due to cyclic pitch motion[1], cyclic in plane air velocity and blades motion, blades perform in a high unsteady aerodynamic environment identical on each revolution. So, the aerodynamic loading F_z^{Aero} applied on a blade is expanded as a Fourier serie at integer multiple of the rotating frequency:

$$\frac{dF_z^{Aero}}{dr} = A_0(r) + \sum_{k=1}^{\infty} \left[A_k(r)\cos\left(k\Omega t\right)\right] \tag{1}$$

where r is the blade radius, $A_k(r)$ corresponds to the spanwise distribution of aerodynamic load at the k^{th} harmonic and Ω is the rotation speed.
This aerodynamic load added with inertial loads due to blade motion are transmitted to fuselage through the hinge. So, loads applied by the i^{th} blade on the hinge are expressed in the rotating frame by:

$$F_z^i = f_{z,0} + \sum_{n=1}^{\infty} \left[f_{z,n}\cos\left(n\Omega t + \frac{2\pi}{b}\left[i-1\right]\right)\right] \tag{2}$$

b corresponds to the number of blades and $f_{z,n}$ is the out-of-plane load applied by blade on the fuselage at the n^{th} harmonic.
This out-of-plane load at the hinge triggers an out-of-plane load F_z^i and an in-plane moment M_y^i at the hub center. After summation of loads from each of the b blades, the transformation from rotating frame to fixed frame gives a vertical load F_z and two in-plane moments M_x and M_y representing the loads applied at the hub center by all blades on fuselage. The expression of vertical load is:

$$F_z = \sum_{i=1}^{b} F_z^i = b\left[f_{z,0} + \sum_{k=1}^{\infty}\left[f_{z,kb}\cos\left(kb\Omega t + \frac{2\pi}{b}(kb-1)\right)\right]\right] \tag{3}$$

The above expression shows that, when an isotropic rotor is considered (rotor tracking and balancing), most of dynamic loads are canceled. Rotor acts as a filter. Only harmonics corresponding to multiples of the number of blades are transmitted to the fuselage [1]. For example, a 5-bladed rotor transmits dynamic loads at 5/rev, 10/rev, 15/rev and so on.

Those dynamic loads, even if limited to $kb\Omega$ harmonics, are responsible for discomfort and alternate stress on components. To limit them, excessive blades responses are avoided by a frequency placement of blade modes. This practical approach needs to be combined with vibration reduction system to ensure a low vibration environment.
Those systems act on vibrations themselves and try to limit them. Numerous passive systems exist which include absorbers and mass-spring systems [2]. Their efficiency is limited, especially with variable rotation speed.
Active vibration control systems are an advanced technique for vibration control, effective on a large frequency band-width and permit to significantly reduce vibration levels [3].
Anyway, active or passive vibration reduction systems bring weight penalty, which has to be avoided.

An alternative way to minimize vibration is to limit dynamic loads at their source, by optimizing the rotor dynamic behavior. Composite blades and their "tailorability" (ability to be designed so that their physical properties meet dynamic requirements) permit to complete this goal.

Composite blade tailoring

Helicopter blades are manufactured with composite materials. Composites, because of their high fatigue properties are well suited to the dynamic environment of the helicopter. Moreover, they present higher corrosion resistance than metal and for the same weight they are stronger and/or stiffer [4], [5] and [6]. Moreover, because of their high modularity, it is possible to tailor their different stiffness properties.
Helicopter blades are composed of different elements. Firstly, a D-spar is used to counter the centrifugal load. A skin covering

[1] It is reminded that pitch corresponds to the rigid rotation along the spanwise axis imposed by the control system, flap is the out-of-plane motion of the blade, lead-lag corresponds to the in-plane motion and torsion deals with the elastic rotation of blade around the spanwise axis.
It is also reminded that the notation $n\Omega$, corresponding to the n^{th} harmonic of rotation speed, is a pulsation and represents an event that occurs n times per revolution (n/rev).

is used to maintain a good aerodynamic shape of the blade section. The core material of both is honeycomb or foam. Spar and skin thickness are chosen because of mechanical properties and frequency considerations. Both are made with composite laminates. Those plies present principal orientation, dicted by fibers orientation. Current blades are made of 0° and $\pm 45^\circ$ carbon laminates. It ensures a quasi-isotropic elastic behavior of the blade. Plies in the spanwise axis contribute to the flexural stiffness of the blade, whereas $\pm 45^\circ$ laminates contribute to the torsional stiffness.

So far, anisotropy of composite materials has not been fully used by helicopter manufacturers. Possibility to tailor the different stiffness properties in torsion and bending are common. Numerous academic studies have been made on blade structural optimization to tailor stiffness, mass and geometric properties. In [7], aeroelastic and sensitivity analyses of the rotor are linked with automated optimization algorithms to perform structural optimization of rotor blades. The objective function constitutes minimization of oscillatory hub loads including constraints on frequency placement, autorotational inertia and aeroelastic stability of the blade in forward flight. More recently, surrogate based optimization methods to tailor structural properties have been developed [8], [9].
Nevertheless, introduction and control of bending-torsion couplings, which potentially improve the dynamic behavior of the blade, has not been done yet on manufactured helicopters.
Those couplings come from aerodynamic, elastic or inertial mechanisms. Inertial and aerodynamic couplings are intrinsec to helicopter blades. Elastic couplings, for their part, are introduced through composite anisotropy and have been avoided by designers because of the lack of tools to fully understand their influence on the blade dynamic behavior. Only one experimental project uses elastically coupled blade in flight: the British Experimental Rotor Program [10], [11]. During this program, a new blade with more performing aerofoils and increased twist than in the previous BERPIII program was used to get higher performances in hover and cruise flights. To keep the same vibratory levels, a structural optimization was performed and elastic couplings were introduced.

The aim of this paper is to understand the influence of flapwise-bending torsion couplings on rotor dynamic loads in order to be able to design a blade which fully takes advantage of the inherent tailorability of composite structures.
A modal approach based on the assumed mode method is used to understand the key mechanisms of such couplings.
Then, their impacts on dynamic loads are studied and a baseline blade improvement is achieved by introducing elastic couplings.

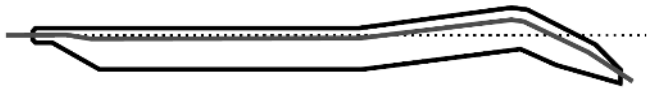

FIGURE 1. Blue Edge^{TM} Planform

FLAPWISE-BENDING TORSION COUPLINGS

Flapwise-bending torsion couplings can occur because of inertial, elastic or aerodynamic phenomena. They are responsible for flutter instability which conduces to the blade destruction.

Aerodynamic and inertial couplings

Aerodynamic couplings occur even with a straight homogeneous blade. The lift load expression dF_z^{Aero} of a portion of section dr, with a chord c, performing in an atmosphere of mass density ρ at the total speed U and presenting a flapwise-bending motion U_z and a torsion motion θ in the case where a linear lift coefficient Cz is considered is:

$$dF_z^{Aero} = \frac{1}{2}\rho c U^2 \frac{dCz}{di}\left[\theta - \frac{\dot{U}_z}{U}\right] dr \tag{4}$$

Lift load acts as a generalized force for the flap modes and for the torsion modes too if there is an offset between aerofoil aerodynamic and torsion centers. The torsion motion modifies the aerodynamic angle of attack and has a direct impact on lift loads which then influence the dynamic behavior of flap and torsion modes. This is the primary source of coupling.

Inertial couplings, for their part, occur because of a chordwise offset between center of gravity and torsion center of section. In new generation blades which present complex planform [12], those couplings are important and inherent to the blade geometry (see figure 1). This complex geometry is due to aeroacoustic and aerodynamic expectations and dynamic requirements are taken into consideration after this aerodynamic definition of blade.

Elastic Couplings

The elastic couplings considered here come from the anisotropic behavior of the composite material. As explained before, the composite blade is composed of a D-spar and a skin covering both made of laminates. Those laminates are made of fibers embedded in an epoxy resin matrix. Fibers can be oriented with an angle from the principal direction of the blade. For a bending-twist coupling, off-axis plies in the upper surface must be parallel to those in the lower one. So, when the blade bends up, upper surface is under compression and lower is strained

by spanwise tension. Due to off-axis plies, those longitudinal stresses trigger shear stresses which act in opposite in plane directions, inducing torsion [5].

When considering an anisotropic beam model with torsion and flapwise-bending only, elastic couplings appear in the matrix of constitutive law as an extra diagonal term K_{45} called "bending-torsion stiffness":

$$\begin{pmatrix} M_t \\ -M_b \end{pmatrix} = \begin{pmatrix} GJ & -K_{45} \\ -K_{45} & EI \end{pmatrix} \begin{pmatrix} \theta' \\ U_z'' \end{pmatrix} \tag{5}$$

This cross coupling stiffness links the flap curvature U_z'' to the torsion moment M_t and the torsion curvature θ' to the flap moment M_b. EI corresponds to the flapwise-bending stiffness and GJ corresponds to the torsional stiffness.
In the case of an articulated rotor, the K_{45} coupling term will have low impact on the aerodynamic performances of the rotor which are dominated by the "rigid" flap mode without curvature. Nevertheless, it is of primary interest when considering higher flap modes which are responsible for dynamic loads. It can be used as a tuning parameter to meet given dynamic requirements.

DYNAMIC BEHAVIOR OF THE COUPLED BLADE

To ensure a fundamental understanding of the influence of couplings on the blade dynamic behavior, blade is supposed to present only flapwise-bending and torsion motions.
Expressions of kinetic energy T and deformation energy U of a coupled flapwise-bending torsion beam with non homogeneous characteristics and undergoing rotations are:

$$U = \frac{1}{2}\int_0^R \left[EI\left(U_z''\right)^2 + GJ\left(\theta'\right)^2 + 2K_{45}U_z''\theta' + F_c\left\{ \left(U_z'\right)^2 + \frac{I_s}{\mu}\left(\theta'\right)^2 \right\} \right] .dr \tag{6}$$

with

$$F_c = \int_x^R \mu r \Omega^2 .dr \tag{7}$$

$$T = \frac{1}{2}\int_0^R \left(\underline{V_G}^2 \mu + \underline{\Omega_s}.\underline{\underline{I_G}}.\underline{\Omega_s} \right) .dr \tag{8}$$

There are no known analytical solutions of this problem, so, an assumed mode method is considered to derive approximated differential equations of motion [13].

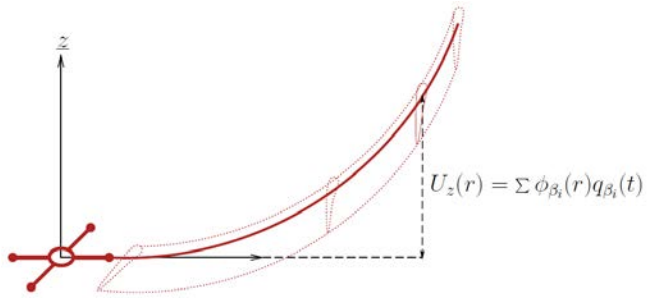

FIGURE 2. Assumed Mode Method

In this approach, small displacements are assumed, and vertical deflection U_z is considered as a superposition of the contribution $q_{\beta i}$ of each flapwise-bending modes $\phi_{\beta i}$ (see figure 2), and torsion θ as a superposition of the contribution $q_{\theta k}$ of each torsion modes $\phi_{\theta k}$:

$$U_z(r) = \sum \phi_{\beta i}(r) q_{\beta i}(t) \qquad \theta(r) = \sum \phi_{\theta k}(r) q_{\theta k}(t) \tag{9}$$

The deformation basis considered in this study comes from the finite element calculation of the uncoupled blade modes [1].
Then, differential equations are derived by applying Lagrange's principle.
This method permits to get results without the need to design a blade cross section precisely. Moreover, it is consistent with other tools already available so as to be integrated in a global dynamic approach. It also ensures a low computation time for preliminary developments.

In the case of only one flapwise-bending mode and one torsion mode in vacuum, the following representation of the linear coupled system, expressed in the uncoupled basis, is obtained:

$$\begin{pmatrix} \mu_\beta & \mu_{\beta\theta} \\ \mu_{\beta\theta} & \mu_\theta \end{pmatrix} \begin{pmatrix} \ddot{q_\beta} \\ \ddot{q_\theta} \end{pmatrix} + \begin{pmatrix} \mu_\beta \omega_\beta^2 & k_{\beta\theta} \\ k_{\beta\theta} & \mu_\theta \omega_\theta^2 \end{pmatrix} \begin{pmatrix} q_\beta \\ q_\theta \end{pmatrix} = \begin{pmatrix} 0 \\ 0 \end{pmatrix} \tag{10}$$

q_β and q_θ refer respectively to the flap modal participation and the torsion modal participation of baseline modes. μ_β and μ_θ are respectively the flap modal mass and the torsion modal mass. ω_β and ω_θ refer respectively to the flap modal pulsation and the torsion modal pulsation. $\mu_{\beta\theta}$ is the inertial coupling between torsion and flapwise-bending dependent on the chordwise offset of the center of gravity:

$$\mu_{\beta\theta} = \int_0^R l_G \phi_\beta \phi_\theta dr \tag{11}$$

ϕ_β and ϕ_θ refer to the flap mode shape and the torsion mode shape.
The stiffness coupling $k_{\beta\theta}$ is studied in the following section.
Moreover, structural damping is not taken into account because for flap and torsion modes, damping comes mainly from the aerodynamic environment.

Coupling strength

When considering the dynamic system coming from Eqn.(10), influence of the flapwise-bending torsion stiffness is seen in the stiffness matrix as an extra diagonal coupling term:

$$k_{\beta\theta} = \int_0^R K_{45}\phi''_\beta\phi'_\theta dr \tag{12}$$

To maximize the coupling between one given torsion mode and one given flap mode, the spanwise distribution of the K_{45} coefficient is of first importance. When considering the 1^{st} torsion mode, which is the mode which couples with flap modes in the advance geometry blade [12], the flap-torsion bending stiffness has to follow the sign of the flap mode curvature to maximize the coupling. So, in the case where the second flap mode is considered, a constant K_{45} is needed. To maximize coupling with higher flap modes, a K_{45} sign changing is needed at different spanwise location. Nevertheless, from a technical point of view, it seems difficult to achieve such a sudden change of sign. That is why, it should be made progressively.
Another important aspect is the amplitude of the K_{45} coefficient. A complete study on the influence of fraction of off-axis plies, spar width and ply orientation angle on bending-torsion stiffness K_{45}, bending stiffness EI and torsional stiffness GJ is given in [5]. Plies in both the skin and the spar in the case of symmetric and antisymmetric laminates are considered. The maximum of coupling is obtained for a plies orientation of 22.5°. When the impact on flexural and torsional stiffness are taken into account a practical limitation of the flapwise-bending torsion stiffness around $0.2\sqrt{EIGJ}$ is obtained. Other authors have worked on this topic and typical optimal values of K_{45} are around 25% of the torsional stiffness.

Effect of structural couplings

When blades rotate in vacuum, only structural coupling occurs. The first effect of this coupling on the dynamic system behavior is the apparition of coupled mode shapes:

$$\hat{W}_{\beta\theta} = \frac{\hat{\omega_\theta}^2 \int l_G.\phi_\beta.\phi_\theta.\mu.dr - \Omega^2 \int l_G.r.\phi'_\beta.\phi_\theta.\mu.dr + \int K_{45}.\phi''_\beta.\phi'_\theta.dr}{\mu_\beta(\omega_\beta^2 - \hat{\omega_\theta}^2)} \tag{13}$$

$$\hat{\tau}_{\beta\theta} = \frac{\hat{\omega_\beta}^2 \int l_G.\phi_\beta.\phi_\theta.\mu.dr - \Omega^2 \int l_G.r.\phi'_\beta.\phi_\theta.\mu.dr + \int K_{45}.\phi''_\beta.\phi'_\theta.dr}{\mu_\theta(\omega_\theta^2 - \hat{\omega_\beta}^2)} \tag{14}$$

The two above coefficients $\hat{W}_{\beta\theta}$ and $\hat{\tau}_{\beta\theta}$ represent respectively the amount of flapwise-bending in the coupled torsion mode and the amount of torsion in the coupled flap mode. They are proportional to the coupling term and inversely proportional to the square of the frequency gap between the two modes.
$\hat{\omega}_\beta$ and $\hat{\omega}_\theta$ refer to the structurally coupled mode frequencies.
If more than two modes are considered in the assumed mode method, and in order to obtain precise coupled mode shapes, it is important to take into consideration more than one torsion mode. Usually, when there are no elastic couplings, only one torsion mode is considered because of its relatively low frequency compared to higher torsion modes. Here, because of the influence of flap curvature on the torsion deformation, more complex torsion shapes appear at lower frequencies, and baseline deformation basis must be more detailed.
In terms of frequency placement, there is a modification due to the flapwise-bending torsion stiffness. Because of the symmetrical behavior of the coupling (see Eqn.(5) and Eqn.(10)), frequency gap between the baseline modes increases and the sign of the elastic coupling has no influence on this frequencies modification.

Effect of aeroelastic couplings

When aerodynamic environment is added to the structurally coupled problem, aeroelastic couplings occur. A good way to understand the influence of the combination of structural and aerodynamic couplings is to express the dynamic system, not in the uncoupled basis but in the structurally coupled basis. The aerodynamic stiffness and damping matrix become:

$$\underline{\underline{\hat{K}}}^{Aéro} = \nu K_{\beta\theta} \begin{pmatrix} \hat{\tau}_{\beta\theta} & 1 \\ \hat{\tau}_{\beta\theta}\hat{W}_{\beta\theta} & \hat{W}_{\beta\theta} \end{pmatrix} \tag{15}$$

$$\underline{\underline{\hat{C}}}^{Aéro} = C_\beta \begin{pmatrix} 1 & \hat{W}_{\beta\theta} \\ \hat{W}_{\beta\theta} & \hat{W}^2_{\beta\theta} \end{pmatrix} \tag{16}$$

$\nu K_{\beta\theta}$ represents the aerodynamic coupling between one flapwise-bending mode and one torsion mode:

$$\nu K_{\beta\theta} = \frac{1}{2}\rho \int_0^R c.U^2.\frac{dC_z}{di}.\phi_\beta.\phi_\theta.dr \tag{17}$$

C_β represents the aerodynamic damping of an uncoupled flapwise-bending mode:

$$C_\beta = -\frac{1}{2}\rho \int_0^R c.U.\frac{dC_z}{di}.{\phi_\beta}^2.dr \tag{18}$$

The first influence of torsional coupling in the flap mode and flap coupling in the torsion mode is a direct aerodynamic stiffness (see Eqn.(15)) . From a physical point of view, it comes from the fact that the torsional component in the coupled flap mode acts as a direct incidence in the expression of the lift load Eqn.(4). For the coupled torsion mode, the flapping shape makes the lift load works. So, even if no aerodynamic offset is considered, the lift load acts as a generalized force for the coupled torsion mode.
The second influence is an indirect stiffness due to the fact that the torsion component of the coupled flap mode acts in the generalized force of the coupled torsion mode. It has an influence on the response of this mode which then impact the generalized force of the coupled flap mode.

Those two stiffening or softening effects have an influence on the frequencies of the aeroelastically coupled modes. This is the principal new effect due to couplings. In the baseline case, there was no frequency effect due to aerodynamic environment, that is why the calculation of uncoupled modes in vaccuum was sufficient to ensure a good frequency placement. When structural couplings exist, the consideration of aerodynamic environment is necessary to correctly evaluate frequencies.
Here, the sign of the structural coupling term $k_{\beta\theta}$ has an influence on the frequency placement. Depending on the ratio between aerodynamic and structural coupling, a sign changing of the bending-torsion stiffness increases or decreases the gap between the baseline frequencies.

IMPACT ON DYNAMIC LOADS

Modal shear loads

A comprehensive way to analyse loads which are transmitted from the rotor to the airframe is to consider modal loads. Flap modes are responsible for vertical shear loads whereas lead-lag modes are responsible for in-plane loads. For an uncoupled flap mode, the expression of the vertical shear load at the n^{th} harmonic is:

$$T_z^{n\Omega} = \frac{{\omega_\beta}^2 Q_\beta \int_0^R \phi_\beta \mu dr}{\mu_\beta (n\Omega)^2 \sqrt{\left[1-\left(\frac{\omega_\beta}{n\Omega}\right)^2\right]^2 + 4{\alpha_\beta}^2\left(\frac{\omega_\beta}{n\Omega}\right)^2}} \tag{19}$$

It depends on the dynamic amplification of the considered mode, which is principally related to the separation between frequencies and rotor harmonics, on the mass repartition and the mode shape, on the modal damping α_β and on the generalized force Q_β applied to the mode.

To highlight the influence of elastic couplings on dynamic loads, the ratio between the shear loads transmitted in the case without elastic couplings $T_z^{n\Omega}$, which corresponds to the usual configuration, and the shear loads in the aeroelastically coupled problem $T_{z_{K_{45}}}^{n\Omega}$, is interesting:

$$R_{T_z}^{n\Omega} = \frac{T_{z_{K_{45}}}^{n\Omega}}{T_z^{n\Omega}} \tag{20}$$

Figure 3 represents the modal shear ratio for the 5^{th} harmonic as a function of the 2^{nd} uncoupled flap mode frequency and the 1^{st} uncoupled torsion mode frequency. Frequency range considered are not representative of a real blade but it allows to easily evaluate general trends of the ratio. The spanwise repartition of K_{45} optimises the coupling between those two modes ($K_{45}^{\beta 2}$), its sign is positive and its amplitude is chosen so as to match 25% of the torsional stiffness GJ.
Areas where a coincidence occurs between the 5^{th} harmonic and the frequencies of uncoupled modes leads to an important modal shear ratio reduction. It is explained on one hand, by a resonance of uncoupled modes due to the zero damping asumption and on the other, by a frequency shift of elastically coupled modes transmissibility. Even if resonance is not reached for elastically coupled modes, an important amplification still occurs so, such a design is not realistic for a low vibration rotor.
This frequency shift of transmissibility is also visible on red areas of the graphic. They correspond to a coincidence between 5^{th} harmonic and coupled mode frequencies.

Concerning general trends of the ratio, areas where $R_{T_z}^{n\Omega}$ is lower than 1 correspond to those where uncoupled frequencies are located on each harmonic side whereas areas where $R_{T_z}^{n\Omega}$ is higher than 1 correspond to those where uncoupled frequencies are on the same harmonic side. This is due to frequencies effect of aeroelastic couplings.
When considering a positive $K_{45}^{\beta 2}$, which is the case here, there is an increase of frequency gap between modes, that is why, a shear load reduction occurs when uncoupled modes are chosen on each side of the harmonic. In contrast, when they are chosen on the same harmonic side, the frequency distancing effect due to coupling leads to a shear load increase.
Here, the elastic coupling sign is important. As it can be seen on figure 4 which represents the variation of modal shear ratio for harmonics 4 and 5 and for $K_{45}^{\beta 2}$ and $K_{45}^{\beta 3}$ as a function of

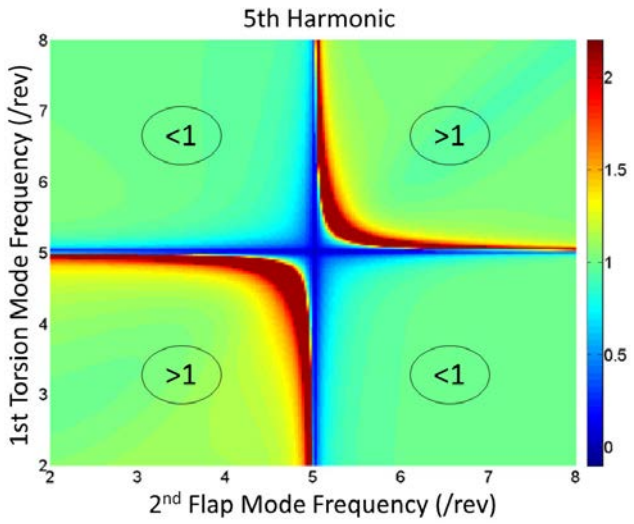

FIGURE 3. MODAL SHEAR RATIO FOR POSITIVE K_{45}

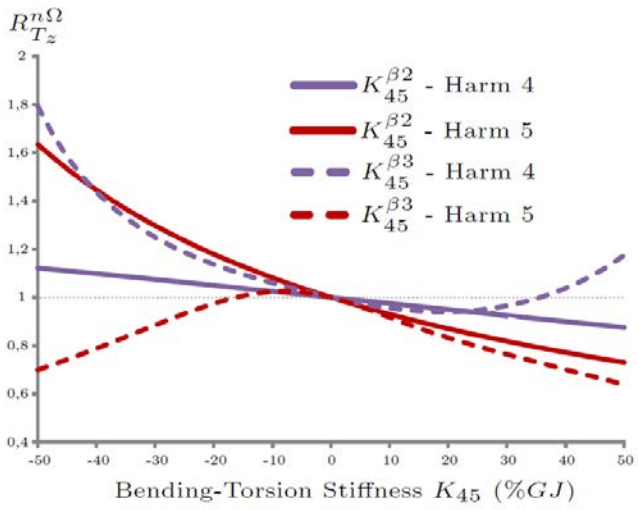

FIGURE 4. MODAL SHEAR RATIO FOR $K_{45}^{\beta 2}$ AND $K_{45}^{\beta 3}$

K_{45} amplitude, a sign modification has influence on the shear loads. Here, uncoupled baseline frequencies are chosen so $\omega_{\beta 2} < 4\Omega < \omega_{\beta 3} < 5\Omega < \omega_{\theta 1}$.
When looking at 5^{th} harmonic, for coupling optimized between 1^{st} torsion mode and 2^{nd} flap mode ($K_{45}^{\beta 2}$), a positive coupling reduce shear loads while a negative one will increase loads. For $K_{45}^{\beta 3}$, conclusion are quite different because, if a certain amount of K_{45} is reached, regarless of the sign, shear loads are reduced.
These behavioral differences come from aerodynamic coupling between modes $\nu K_{\beta\theta}$. For 2^{nd} flap mode and 1^{st} torsion mode, this coupling is very important and adding elastic coupling, according to their sign, will counter or amplify the frequency effects due to aerodynamic coupling. Whereas, for the 3^{rd} flap mode and 1^{st} torsion mode, aerodynamic coupling is small and, for a sufficient amount of elastic coupling, aerodynamic effects are "erased". As if it were in vacuum, whatever the coupling sign is, frequency gap between modes increases, resulting in a load reduction.
Difference between harmonic 4 and 5 are due, once again, to modes frequency distribution with respect to the harmonic.

Dynamic improvement of a baseline blade

The aim of this section is to improve the dynamic behavior of a baseline blade by adding elastic couplings and by modifying the 1^{st} torsion mode frequency, in order to minimize dynamic loads transmitted from the rotor at 5/rev.
To this end, a simplified uniform blade is considered. Its "initial" flapping and torsional frequencies are listed in table 1.

TABLE 1. BASELINE BLADE FREQUENCIES (/REV)

Flap1	Flap2	Flap3	Torsion1	Flap4	Flap5	Torsion2
1.04	2.62	4.56	4.85	6.96	9.97	15.37

As explained previously, elastic couplings impact frequencies because of the air softening or stiffening effect due to coupled shape modes. Here, effects on dynamic loads will be considered through the impact of couplings on the frequency placement in the aerodynamic environment.
A linear modal approach, similar to the previous one, is considered with five flap modes and two torsion modes.

When looking at the table 1, the proximity of the 1^{st} torsion mode and the 3^{rd} flapwise bending mode with the 5/rev indicates that a well-designed coupling between those two modes will have an important impact on dynamic loads.
Figures 5 shows the difference between coupled frequencies and baseline frequencies as functions of K_{45} in the case where it is optimized for a coupling between 1^{st} torsion mode and 3^{rd} flapping mode.
As expected, the most important frequencies modifications occur for the targeted modes. Nevertheless, other frequencies are modified too. 2^{nd} and 4^{th} flapping modes and 2^{nd} torsion mode are impacted. This is due to the fact that an optimized K_{45} distribution, chosen to maximize coupling between two targeted modes, has no reason to minimize couplings with other modes.

On most of the $K_{45}^{\beta 3}$ range considered here, there is an

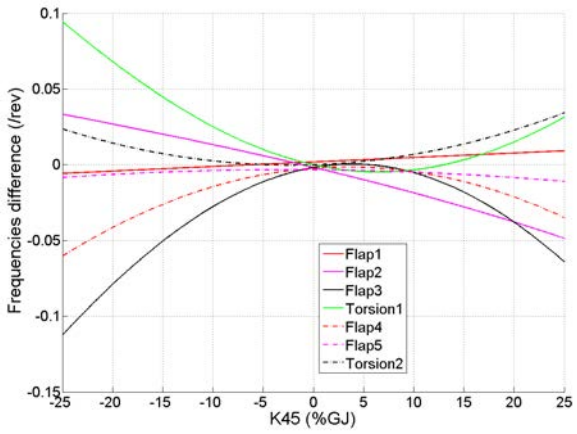

FIGURE 5. FREQUENCIES DIFFERENCE BETWEEN COUPLED AND BASELINE MODES FOR $K_{45}^{\beta 3}$ VARIATION

increase of the gap between the 3^{rd} flapwise bending mode frequency and the 1^{st} torsion mode frequency. The maximum of coupling effect is obtained for a negative bending-torsion stiffness of 25% of the torsional stiffness. The problem is that, initially, those modes where on the same side of the 5^{th} harmonic (see table.1). So, this coupling will result in increased shear loads.

Knowing that elastic couplings increase the frequency gap between the two modes of interest, a load reduction can be achieved by setting the 1^{st} uncoupled torsion mode frequency above the harmonic of interest so that the increase of the gap between modes frequencies results in an increase of the gap between modes frequencies and harmonic. This can be easily done, without altering blade properties, by stiffening the pich control system.

Nevertheless, such a design change must be validated by verifying that flutter margins are maintained.

Stability When dealing with vibration reduction issues, designer must keep in mind stability criterions. Aeroelastic couplings can increase or decrease margins and the verification that the chosen design is still stable is of first importance.

Usually, uncoupled torsion modes present low damping. So, coupling with flapwise-bending modes must be chosen to bring damping in order to avoid divergence.

When looking at the figures 6 and 7, representing modal dampings as functions of the 1^{st} torsion mode frequency in the case of a positive and a negative $K_{45}^{\beta 3}$ of 25% of GJ, instability occurs only for the positive coupling case and for a torsion frequency lower than $4.5/rev$.

In the portion of interest, i.e for torsion frequencies higher than

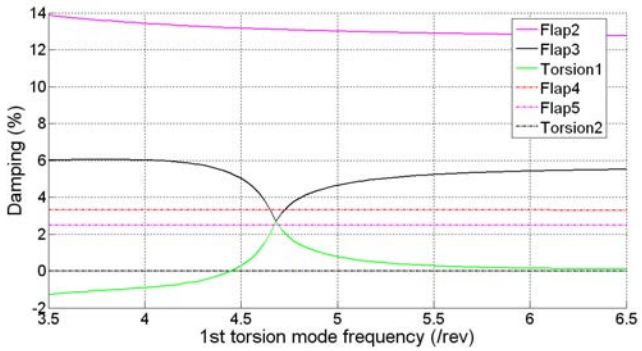

FIGURE 6. DAMPING FOR $\omega_{\theta 1}$ VARIATIONS FOR A POSITIVE $K_{45}^{\beta 3}$

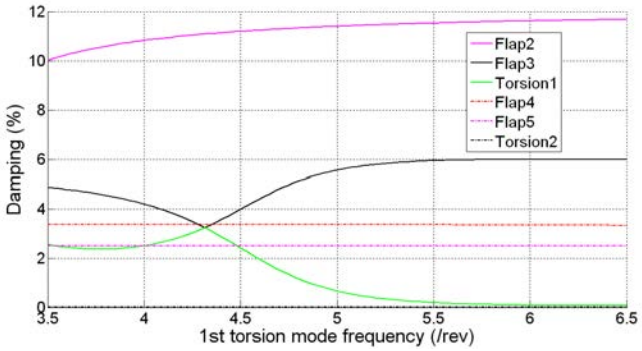

FIGURE 7. DAMPING FOR $\omega_{\theta 1}$ VARIATIONS FOR A NEGATIVE $K_{45}^{\beta 3}$

$5/rev$, system is still stable.

Finally, when dynamic loads and stability requirements are taken into account, a design which maximizes the coupling effect, while reducing modal shear loads and keeping good stability margins is obtained with a negative $K_{45}^{\beta 3}$ of $25\%GJ$ with an uncoupled torsion frequency near $5.2/rev$.

Tailoring rules - Conclusions

According to previous analysis, some tailoring rules can be enonciated. Some comparisons can be made with conclusions outlined in reference [11].

Firstly, to maximize coupling, K_{45} must be designed so as to fit the flap mode of interest. For a coupling with the 1^{st} torsion mode, the K_{45} spanwise distribution must be close to the flap mode curvature. Nevertheless, an optimized bending-torsion stiffness for one given flap mode does not guarantee a minimum

of coupling with other flap modes.
Moreover, technical issues must be investigated to know the practical limits of K_{45} and of its distribution along the spanwise axis.

Secondly, torsion and flap modes must be adapted so as to be close in terms of frequencies. It increases the coupling effect and permits to obtain coupled modes with both torsional and flapping important contributions which acts on generalized aerodynamic loads and triggers an aerodynamic stiffening or softening effect.
One way to modify torsion frequency is to act on the pitch control system stiffness. This allows to "tailor" the blade dynamic behavior without altering blade properties.
Flapwise-bending modes frequencies are harder to adapt because only a change in mass or stiffness generates frequency change, and these parameters are structurally related.
This adaptation must be performed carefully in order to keep adequate stability margins.

Thirdly, introducing coupling is more efficient for uncoupled flap modes initially close to the harmonic of interest. Even if those designs are most of the time avoided for uncoupled blades, it enables to maximize the dynamic amplification shift effect due to coupling.

Fourthly, according to the aerodynamic coupling intensity between modes of interest, elastic coupling sign and magnitude must be selected so as to generate a frequency spacing, and modes of interest must be chosen on both sides of the targeted harmonic. It ensures an increase of the frequency gap between elastically coupled modes frequencies and the harmonic.

Finally, stability criterions must be kept in mind and blade must be tailored under stability constraints to ensure viable designs.

REFERENCES

[1] Cranga, P., 2005. "Comportement dynamique de l'hélicoptère - contribution à la définition de l'architecture générale". PhD thesis, INSA de Lyon.

[2] Cranga, P., and Aubourg, P.-A., 2008. "Recent advances in eurocopters passive and active vibration control". In American Helicopter Society 64th Annual Forum, Montral, Canada, April 29 May 1, p. 18.

[3] Priems, M., Dreher, S., Konstanzer, P., Hoffmann, F., Kerdreux, B., and Jouve, J., 2012. "Active cabin vibration control for light single and twin engine helicopters". In American Helicopter Society 68th.

[4] Floros, M. W., 2000. "Elastically tailored composite rotor blades for stall alleviation and vibration reduction". PhD thesis, The Pennsylvania State University.

[5] Piatak, D. J., 1997. Stiffness characteristics of composite rotor blades with elastic coupling. Tech. rep., NASA.

[6] Ganguli, R., and Chopra, I., 1997. "Aeroelastic tailoring of composite couplings and blade geometry of a helicopter rotor using optimization methods". *Journal of the American Helicopter Society,* ***42***(3), pp. 218–228.

[7] Ganguli, R., and Chopra, I., 1996. "Aeroelastic optimization of an advanced geometry helicopter rotor". *Journal of the American Helicopter Society,* ***41***(1), pp. 18–28.

[8] Glaz, B., Friedmann, P., and Liu, L., 2008. "Surrogate based optimization of helicopter rotor blades for vibration reduction in forward flight". *Structural and Multidisciplinary Optimization,* ***35***, pp. 341–363. 10.1007/s00158-007-0137-z.

[9] Ganguli, R., 2002. "Optimum design of a helicopter rotor for low vibration using aeroelastic analysis and response surface methods". *Journal of Sound and Vibration,* ***258***, p. 327344.

[10] Harrison, R., Stacey, S., and Hansford, B., 2008. "Berp iv the design, development and testing of an advanced rotor blade". In American Helicopter Society 64th Annual Forum, Montral, Canada, April 29 May 1.

[11] Moffatt, S., and Griffiths, N., 2009. "Structural optimisation and aero-elastic tailoring of the berp iv demonstrator blade". In American Helicopter Society 65th Annual Forum, Grapevine, Texas, May 27-29.

[12] Skladanek, Y., 2011. "Formulation d´un Élément fini de poutre pour la dynamique des pales d´hélicoptère de géométrie complexe". PhD thesis, INSA Lyon.

[13] A. R. S. Bramwell, G. D., and Balmford, D., 2001. *Bramwells Helicopter Dynamics*. Butterworth-Heinemann.